

NLO QCD corrections to hadronic $W^+W^-b\bar{b}$ production

Stefano Pozzorini*

Institut für Theoretische Physik, Universität Zürich, 8057 Zürich, Switzerland

E-mail: pozzorin@physik.uzh.ch

Ansgar Denner

Universität Würzburg, Institut für Theoretische Physik und Astrophysik, 97074 Würzburg, Germany

E-mail: denner@physik.uni-wuerzburg.de

Stefan Dittmaier

Albert-Ludwigs-Universität Freiburg, Physikalisches Institut, 79104 Freiburg, Germany

E-mail: stefan.dittmaier@physik.uni-freiburg.de

Stefan Kallweit

Institut für Theoretische Physik, Universität Zürich, 8057 Zürich, Switzerland

E-mail: kallweit@physik.uzh.ch

We report on the calculation of the NLO QCD corrections to hadronic $W^+W^-b\bar{b}$ production. This provides a full NLO description of top-pair production and decay, including interferences, off-shell effects, non-resonant diagrams, as well as leptonic W-boson decays. We discuss results for the Tevatron and the LHC, with emphasis on finite-width effects of the top quarks and distortions of kinematic distributions.

10th International Symposium on Radiative Corrections (Applications of Quantum Field Theory to Phenomenology)

September 26-30, 2011

Mamallapuram, India

*Speaker.

1. Introduction

Top-quark pair production at hadron colliders allows for key tests of the Standard Model and represents an omnipresent background to new physics. The very large $t\bar{t}$ samples from the Tevatron and the LHC, and the steadily increasing systematic precision, call for a continuous improvement of theory predictions. Besides the next-to-leading-order (NLO) QCD corrections [1, 2, 3, 4], also the electroweak corrections to hadronic $t\bar{t}$ production are well known [5, 6, 7, 8, 9]. Present research focuses on resummation of logarithmically enhanced terms [10, 11, 12, 13, 14, 15, 16] and on the completion of the next-to-next-to-leading-order QCD corrections [17, 18, 19, 20, 21, 22, 23, 24, 25, 26, 27, 28, 29]. Another important aspect is the precise theoretical simulation of experimental cuts and exclusive $t\bar{t}$ observables, which depend on details of the $W^+W^-b\bar{b}$ decay products. A first step towards full NLO predictions for hadronic $W^+W^-b\bar{b}$ production was done in Refs. [30, 31, 32], where on-shell top-pair production was complemented by NLO top-quark decays in spin-correlated narrow-width approximation. More recently, complete NLO predictions for $pp \rightarrow W^+W^-b\bar{b} + X$ became available [33, 34], where also off-shell top quarks and non-resonant diagrams are included. In these proceedings we report on the calculation of Ref. [33]. In the context of NLO calculations for multi-particle processes at hadron colliders [35], $pp \rightarrow W^+W^-b\bar{b}$ is the first $2 \rightarrow 4$ particle process that involves intermediate unstable particles. For a consistent treatment of the top-quark resonances we adopt the complex-mass scheme, which was introduced at the NLO level in the framework of the calculation of the electroweak corrections to $e^+e^- \rightarrow WW \rightarrow 4$ fermions [36, 37].

At leading order (LO), hadronic $W^+W^-b\bar{b}$ production proceeds via $q\bar{q}$ and gg partonic channels. Our calculation involves doubly-resonant (DR) contributions with $t\bar{t}$ intermediate states, channels with a single (anti)top resonance, and non-resonant contributions. The widely used narrow-width approximation, which includes only DR contributions with on-shell top quarks, corresponds to the $\Gamma_t \rightarrow 0$ limit of our calculation. The additional contributions—from off-shell top quarks and singly- or non-resonant channels—are expected to be $\mathcal{O}(\Gamma_t/m_t)$ suppressed in inclusive observables. Their calculation becomes important for percent-level precision in $t\bar{t}$ observables and for a reliable simulation of $W^+W^-b\bar{b}$ backgrounds in Higgs and new-physics searches, where off-shell effects can be enhanced by $t\bar{t}$ -suppressing cuts. To describe top-quark decays in a realistic way we include the leptonic W-boson decays $W^+ \rightarrow \nu_e e^+$ and $W^- \rightarrow \bar{\nu}_\mu \mu^-$ in spin-correlated narrow-width approximation.

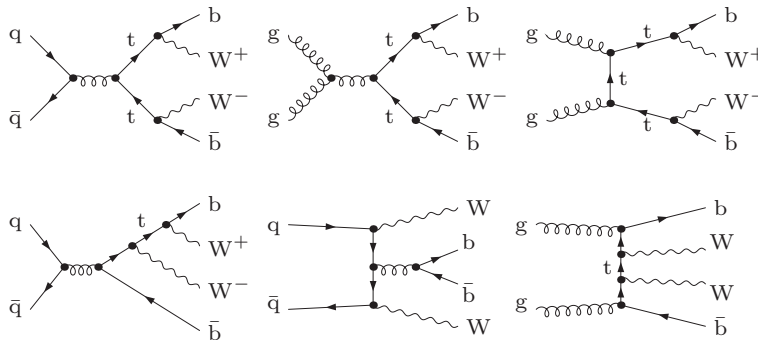


Figure 1: Representative LO diagrams of doubly-resonant (upper line), singly-resonant (first diagram in lower line), and non-resonant type (last two diagrams in lower line).

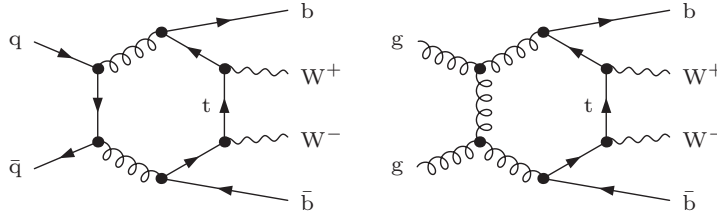


Figure 2: Examples of rank-4 and rank-5 hexagon diagrams in the $q\bar{q}/gg \rightarrow W^+W^-b\bar{b}$ channels.

2. Technical aspects of the calculation

The one-loop $q\bar{q}/gg \rightarrow W^+W^-b\bar{b}$ amplitudes are computed using Feynman diagrams and tensor integrals. The latter are reduced to scalar integrals adopting the numerically stable techniques of Refs. [38, 39]. The $q\bar{q}$ and gg channels comprise about 300 and 800 one-loop diagrams, respectively (see Fig. 2). Hexagon and pentagon diagrams reach tensor rank up to five in the gg channel. Feynman diagrams are generated with FEYNARTS [40, 41], and one-loop amplitudes are reduced along the lines of Refs. [42, 43]. The employed approach strongly mitigates the complexity inherent in Feynman diagrams, and the reduced algebraic expressions are automatically converted into very fast FORTRAN code. The evaluation of the virtual corrections in the gg channel, including helicity and colour sums, takes roughly 200 ms per phase-space point.¹ The size of the executable program (dominated by the one-loop corrections) ranges from 0.25 to 1.2 GB, depending on the details of the algebraic reduction and the applied compilers.

To regularise top resonances we employ the gauge-invariant complex-mass scheme [37]. The top-quark width Γ_t is incorporated into the definition of the renormalised squared top-quark mass, $\mu_t^2 = m_t^2 - im_t\Gamma_t$, which is identified with the position of the pole of the top-quark propagator in the complex plane. This requires one-loop scalar box integrals with complex masses, for which we use the general analytic continuations presented in Ref. [44].

The real corrections receive contributions from the $2 \rightarrow 5$ partonic processes $gg \rightarrow W^+W^-b\bar{b}g$ and $q\bar{q} \rightarrow W^+W^-b\bar{b}g$, as well as from crossing-related gq and $g\bar{q}$ channels. The $2 \rightarrow 5$ matrix elements are evaluated with MADGRAPH [45] and, alternatively, using the Weyl–van-der-Waerden formalism of Ref. [46]. To isolate infrared divergences and cancel them analytically we employ in-house implementations of the dipole subtraction formalism [47, 48]. Colour and helicity correlations that enter the subtraction procedure are generated by means of AUTODIPOLE [49] and, alternatively, in analytic form.

3. Selected numerical results for the Tevatron and the LHC

In the following we discuss NLO predictions for $W^+W^-b\bar{b}$ production with leptonic W -boson decays at the Tevatron and the 7 TeV LHC. Hadronic observables are obtained with the MSTW2008 set of parton distributions [50], and details on input parameters can be found in Ref. [33]. Among the various parameters, the top-quark decay width plays a special role. On the one hand, Γ_t enters

¹The CPU performance can vary by a factor two or so, depending on the processor and the compiler. Using a single Intel i5-750 core and the ifort 10.1. compiler we measured a speed of 180 ms per point.

the two top-quark propagators and leads to a $1/\Gamma_t^2$ dependence of the cross section in the narrow-width limit. On the other hand, the integration of the resonant matrix elements over the top-quark decay products yields a related factor $(\Gamma_{t \rightarrow b\nu})^2$, so that the total cross section in the narrow-width limit is proportional to the (squared) branching ratio

$$\text{BR}(t \rightarrow b\nu) = \frac{\Gamma_{t \rightarrow b\nu}}{\Gamma_t}. \quad (3.1)$$

In order to obtain a consistent definition of this branching ratio, the partial widths of all top-decay processes contributing at the given perturbative level must sum up to Γ_t . To guarantee this, the top decay width and all matrix elements must be computed with the same input parameters and approximations and, of course, at the same perturbative order. Due to the Γ_t^{-2} dependence of the cross section, small inconsistencies in the choice of Γ_t can have a non-negligible impact. Our LO and NLO predictions are obtained using $m_t = 172 \text{ GeV}$ and the top-quark widths $\Gamma_{t,\text{LO}} = 1.4655 \text{ GeV}$ and $\Gamma_{t,\text{NLO}} = 1.3376 \text{ GeV}$ [51], respectively. Since the leptonic W-boson decay does not receive NLO QCD corrections we employ the NLO W-boson width $\Gamma_W = 2.0997 \text{ GeV}$ everywhere. As mentioned in the introduction, in contrast to top-quark decays, W-boson decays are treated in the narrow-width limit. In this respect, we point out that finite W-width effects are expected to be doubly suppressed. This becomes clear if one considers that, in the $\Gamma_t \rightarrow 0$ limit, the $W^+W^-b\bar{b}$ cross section is proportional to the squared branching ratio (3.1), where $\mathcal{O}(\Gamma_W)$ corrections to the numerator and denominator cancel. Finite W-width corrections are thus expected to produce very small effects of $\mathcal{O}(\frac{\Gamma_W \Gamma_t}{M_W m_t})$ in inclusive observables.

We convert QCD partons into jets with the anti- k_T algorithm [52] using $R = 0.4(0.5)$ at the Tevatron (LHC). Standard $t\bar{t}$ signal cuts are applied: $p_{T,b} > 20(30) \text{ GeV}$ and $|\eta_b| < 2.5$ for b-jets, $p_{T,\text{miss}} > 25(20) \text{ GeV}$, and $p_{T,l} > 20 \text{ GeV}$, $|\eta_l| < 2.5$ for charged leptons. For the renormalisation and factorisation scales we adopt the central value $\mu = m_t$ and study factor-2 variations of $\mu = \mu_{\text{ren}} = \mu_{\text{fact}}$. At the Tevatron, where the cross section is dominated by the $q\bar{q}$ channel, at $\mu = m_t$ we obtain $\sigma_{\text{LO}}^{\text{TeV}} = 44.31^{+19.68}_{-12.49} \text{ fb}$ and $\sigma_{\text{NLO}}^{\text{TeV}} = 41.75^{+0.00}_{-3.79} \text{ fb}$, where the errors describe $m_t/2 < \mu < 2m_t$ variations. For the LHC, where the gg channel dominates, we obtain $\sigma_{\text{LO}}^{\text{LHC}} = 662.4^{+263.4}_{-174.1} \text{ fb}$ and $\sigma_{\text{NLO}}^{\text{LHC}} = 840^{+27}_{-75} \text{ fb}$. Normalising the results to LO predictions at $\mu = m_t$ we obtain the relative NLO corrections $K^{\text{TeV}} = 0.942^{+0.000}_{-0.085}$ and $K^{\text{LHC}} = 1.27^{+0.04}_{-0.11}$. The NLO corrections induce a moderate shift of the integrated cross section and reduce its scale uncertainty from about 44% (40%) to 9% (9%) at the Tevatron (LHC). This corresponds to the usual picture emerging from NLO calculations of the inclusive $t\bar{t}$ cross section at hadron colliders. The K factors obtained in the independent $W^+W^-b\bar{b}$ calculation of Ref. [34] deviate quite significantly from the ones reported above. This is due to differences in the choice of input parameters, cuts, and PDFs. In a tuned comparison, in collaboration with the authors of Ref. [34], it was found that the integrated NLO cross section at the Tevatron agrees at the permille precision level.

To quantify non-resonant and off-shell contributions to the $W^+W^-b\bar{b}$ integrated cross section, we investigated its narrow-width limit, $\Gamma_t \rightarrow 0$, by means of a numerical extrapolation. This is shown in Fig. 3, where we plot $\sigma_{W^+W^-b\bar{b}}(\Gamma_t) \times (\Gamma_t/\Gamma_t^{\text{phys}})^2$ for increasingly small numerical values of Γ_t . The top-quark width Γ_t is handled as a free parameter, and the factor $(\Gamma_t/\Gamma_t^{\text{phys}})^2$ compensates for deviations of the squared branching fraction from its Standard Model value. In the $\Gamma_t \rightarrow 0$ limit, the virtual and real parts of NLO corrections are individually enhanced by soft-gluon loga-

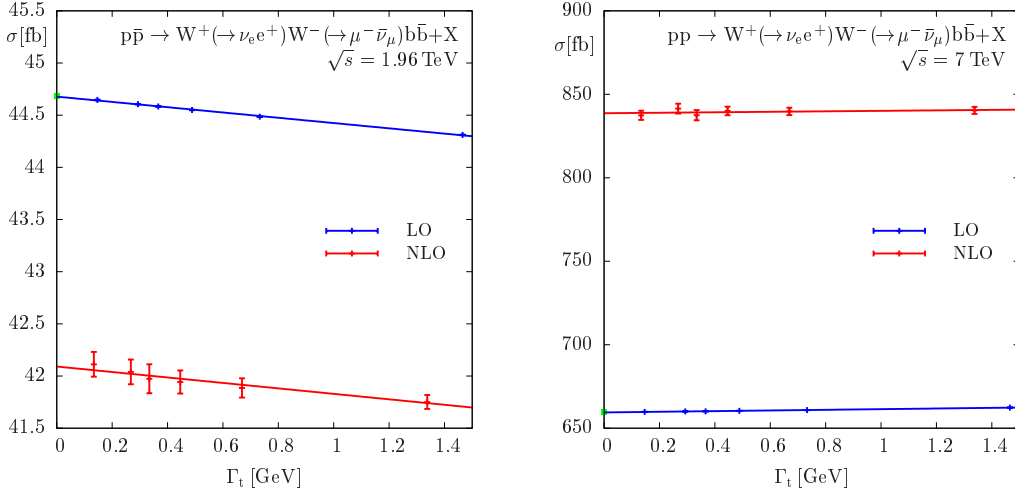


Figure 3: Numerical narrow-width extrapolation of the LO and NLO $W^+W^-b\bar{b}$ cross section at the Tevatron and the LHC.

rithmic singularities, which are not subtracted via Catani-Seymour dipoles. The precise numerical cancellation of such singularities in the sum of virtual and real corrections manifests itself in the quality of the linear convergence of the $\Gamma_t \rightarrow 0$ extrapolation. This provides a nontrivial confirmation of the consistency and numerical stability of the calculation. Non-resonant and off-shell effects are extracted by comparing results at $\Gamma_t = \Gamma_t^{\text{phys}}$ and $\Gamma_t \rightarrow 0$. At the Tevatron, finite-width effects shift the LO(NLO) cross section by -0.8% (-0.9%). This is fairly close to the numerical value of Γ_t/m_t , which represents the expected order of magnitude. At the LHC, finite-width effects turn out to be even smaller: $+0.4\%$ at LO and $+0.2\%$ (comparable to the Monte Carlo statistical error) at NLO. The suppression of finite-width effects at the LHC might be due to cancellations between positive non-resonant contributions and negative off-shell corrections.

As an example of the kinematic dependence of NLO corrections, in Fig. 4 we plot the charged-lepton p_T -distribution at the LHC. The typical lepton p_T is below 100 GeV. In the plotted range, the cross section falls by two orders of magnitude, and the K factor exhibits a rather strong p_T sensitivity with up to 30% variation. This is especially relevant at large p_T , and to stabilise LO predictions it might be useful to employ a dynamical QCD scale.

In Fig. 5 we display NLO and finite-width corrections to the invariant-mass distribution of the positron and the corresponding b-jet—the visible products of the top-quark decay—at the Tevatron. In narrow-width and LO approximation this kinematic quantity is characterised by a sharp upper bound, $M_{e+b}^2 \leq m_t^2 - M_W^2$, which renders it very sensitive to the top-quark mass. NLO corrections to this observable in narrow-width approximation have been discussed in Ref. [53]. A related observable—the invariant-mass distribution of a positron and a J/ψ from a B -meson decay—can be exploited for a high-precision determination of m_t at the LHC [54]. Fig. 5 shows small but non-negligible off-shell contributions that elude the kinematic bound already in LO. At NLO this feature becomes more pronounced, also due to QCD radiation that enters the b-jet without being emitted from its parent bottom quark. Below the kinematic bound, where we find the bulk of the cross section, NLO effects are quite important. In the range $50 \text{ GeV} < M_{e+b} < 150 \text{ GeV}$ the shape

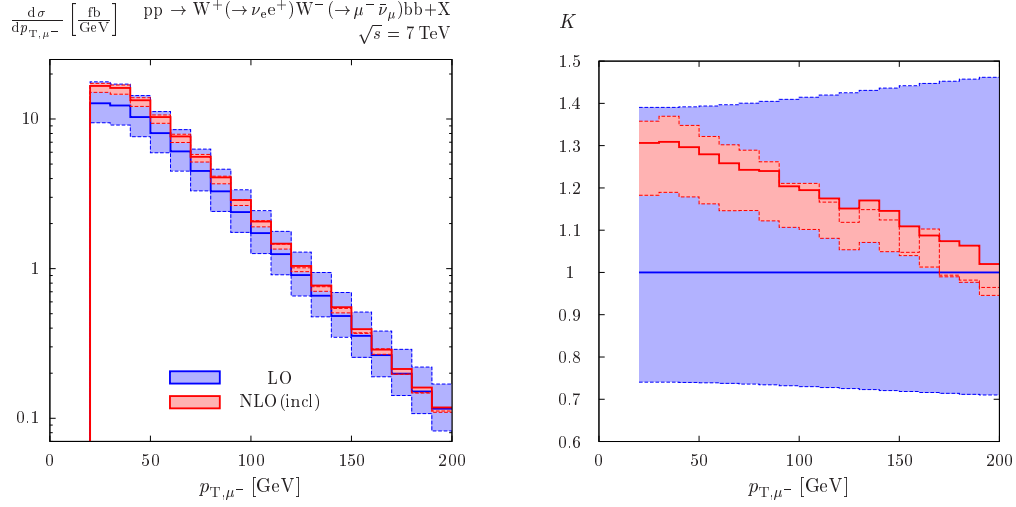


Figure 4: Charged-lepton transverse-momentum distribution at the LHC: absolute LO and NLO predictions (left) and relative corrections w.r.t. LO at $\mu = m_t$ (right). The uncertainty bands describe $m_t/2 < \mu < 2m_t$ scale variations.

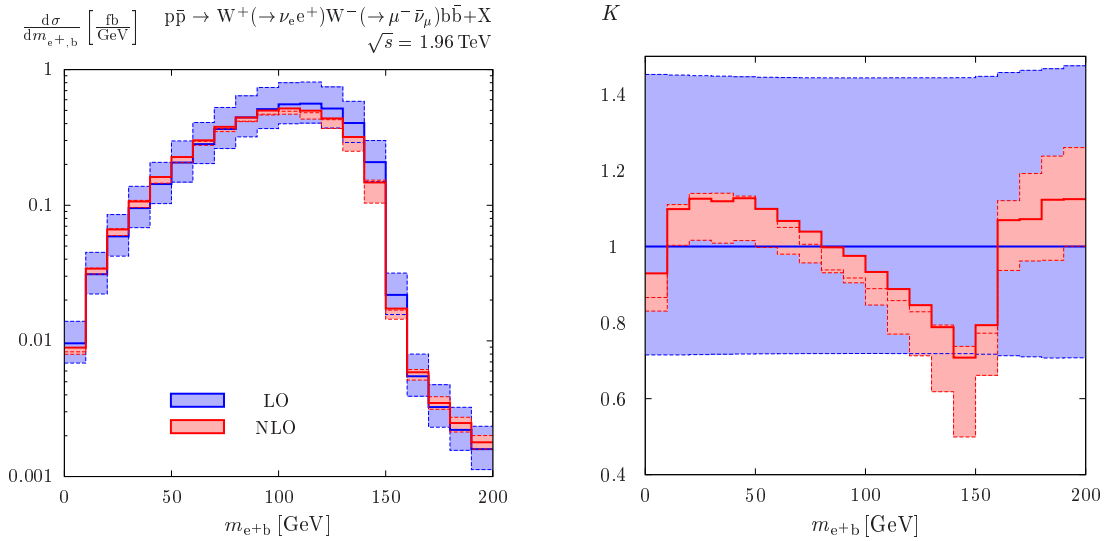


Figure 5: Invariant mass M_{e+b} of the positron-b-jet system at the Tevatron: absolute LO and NLO predictions (left) and relative corrections w.r.t. LO at $\mu = m_t$ (right). The uncertainty bands describe $m_t/2 < \mu < 2m_t$ scale variations.

of M_{e+b} is strongly distorted, and the corrections vary between +15% and -30% (see right plot).

These results demonstrate the importance of NLO predictions for a precise simulation of the kinematic details of $W^+W^-b\bar{b}$ signatures at hadron colliders.

Acknowledgments

S.P. thanks the Swiss National Science Foundation for support. This work was supported in part by the Research Executive Agency (REA) of the European Union under the Grant Agreement number PITN-GA-2010-264564 (LHCPhenoNet).

References

- [1] P. Nason *et. al.*, *Nucl. Phys.* **B327** (1989) 49–92.
- [2] W. Beenakker *et. al.*, *Nucl. Phys.* **B351** (1991) 507–560.
- [3] M. L. Mangano, P. Nason, and G. Ridolfi, *Nucl. Phys.* **B373** (1992) 295–345.
- [4] S. Frixione *et. al.*, *Phys. Lett.* **B351** (1995) 555–561, [hep-ph/9503213].
- [5] W. Beenakker *et. al.*, *Nucl. Phys.* **B411** (1994) 343–380.
- [6] S. Moretti, M. R. Nolten, and D. A. Ross, *Phys. Lett.* **B639** (2006) 513–519, [hep-ph/0603083].
- [7] J. H. Kühn, A. Scharf, and P. Uwer, *Eur. Phys. J.* **C51** (2007) 37–53, [hep-ph/0610335].
- [8] W. Bernreuther, M. Fückler, and Z.-G. Si, *Phys.Rev.* **D74** (2006) 113005, [hep-ph/0610334].
- [9] W. Bernreuther, M. Fückler, and Z.-G. Si, *Nuovo Cim.* **B123** (2008) 1036–1044, [arXiv:0808.1142].
- [10] M. Beneke, P. Falgari, and C. Schwinn, *Nucl. Phys.* **B828** (2010) 69–101, [arXiv:0907.1443].
- [11] M. Beneke, P. Falgari, S. Klein, and C. Schwinn, *Nucl.Phys.* **B855** (2012) 695–741, [arXiv:1109.1536].
- [12] M. Czakon, A. Mitov, and G. F. Sterman, *Phys. Rev.* **D80** (2009) 074017, [arXiv:0907.1790].
- [13] M. Cacciari *et. al.*, arXiv:1111.5869.
- [14] V. Ahrens *et. al.*, *JHEP* **1009** (2010) 097, [arXiv:1003.5827].
- [15] V. Ahrens *et. al.*, arXiv:1103.0550.
- [16] N. Kidonakis, *Phys.Rev.* **D82** (2010) 114030, [arXiv:1009.4935].
- [17] S. Dittmaier, P. Uwer, and S. Weinzierl, *Phys. Rev. Lett.* **98** (2007) 262002, [hep-ph/0703120].
- [18] B. Kniehl *et. al.*, *Phys. Rev.* **D78** (2008) 094013, [arXiv:0809.3980].
- [19] C. Anastasiou and S. M. Aybat, *Phys. Rev.* **D78** (2008) 114006, [arXiv:0809.1355].
- [20] M. Czakon, A. Mitov, and S. Moch, *Phys. Lett.* **B651** (2007) 147–159, [arXiv:0705.1975].
- [21] M. Czakon, A. Mitov, and S. Moch, *Nucl. Phys.* **B798** (2008) 210–250, [arXiv:0707.4139].
- [22] M. Czakon, *Phys. Lett.* **B664** (2008) 307–314, [arXiv:0803.1400].
- [23] R. Bonciani *et. al.*, *JHEP* **07** (2008) 129, [arXiv:0806.2301].

- [24] R. Bonciani *et. al.*, *JHEP* **0908** (2009) 067, [arXiv:0906.3671].
- [25] R. Bonciani *et. al.*, *JHEP* **1101** (2011) 102, [arXiv:1011.6661].
- [26] M. Czakon, *Phys. Lett.* **B693** (2010) 259–268, [arXiv:1005.0274].
- [27] G. Abelof and A. G.-D. Ridder, arXiv:1112.4736.
- [28] M. Czakon, *Nucl.Phys.* **B849** (2011) 250–295, [arXiv:1101.0642].
- [29] I. Bierenbaum, M. Czakon, and A. Mitov, *Nucl.Phys.* **B856** (2012) 228–246, [arXiv:1107.4384].
- [30] W. Bernreuther *et. al.*, *Nucl. Phys.* **B690** (2004) 81–137, [hep-ph/0403035].
- [31] K. Melnikov and M. Schulze, *JHEP* **08** (2009) 049, [arXiv:0907.3090].
- [32] W. Bernreuther and Z.-G. Si, *Nucl. Phys.* **B837** (2010) 90–121, [arXiv:1003.3926].
- [33] A. Denner *et. al.*, *Phys.Rev.Lett.* **106** (2011) 052001, [arXiv:1012.3975].
- [34] G. Bevilacqua *et. al.*, *JHEP* **1102** (2011) 083, [arXiv:1012.4230].
- [35] **SM and NLO Multileg Working Group** Collaboration, J. R. Andersen *et. al.*, arXiv:1003.1241.
- [36] A. Denner *et. al.*, *Phys. Lett.* **B612** (2005) 223–232, [hep-ph/0502063].
- [37] A. Denner *et. al.*, *Nucl. Phys.* **B724** (2005) 247–294, [hep-ph/0505042].
- [38] A. Denner and S. Dittmaier, *Nucl. Phys.* **B658** (2003) 175–202, [hep-ph/0212259].
- [39] A. Denner and S. Dittmaier, *Nucl. Phys.* **B734** (2006) 62–115, [hep-ph/0509141].
- [40] J. Küblbeck, M. Böhm, and A. Denner, *Comput. Phys. Commun.* **60** (1990) 165–180.
- [41] T. Hahn, *Comput. Phys. Commun.* **140** (2001) 418–431, [hep-ph/0012260].
- [42] A. Bredenstein *et. al.*, *JHEP* **08** (2008) 108, [arXiv:0807.1248].
- [43] A. Bredenstein *et. al.*, *JHEP* **1003** (2010) 021, [arXiv:1001.4006].
- [44] A. Denner and S. Dittmaier, *Nucl. Phys.* **B844** (2011) 199–242, [arXiv:1005.2076].
- [45] J. Alwall *et. al.*, *JHEP* **09** (2007) 028, [arXiv:0706.2334].
- [46] S. Dittmaier, *Phys. Rev.* **D59** (1999) 016007, [hep-ph/9805445].
- [47] S. Catani and M. H. Seymour, *Nucl. Phys.* **B485** (1997) 291–419, [hep-ph/9605323].
- [48] S. Catani *et. al.*, *Nucl. Phys.* **B627** (2002) 189–265, [hep-ph/0201036].
- [49] K. Hasegawa, S. Moch, and P. Uwer, *Comput. Phys. Commun.* **181** (2010) 1802–1817, [arXiv:0911.4371].
- [50] A. D. Martin *et. al.*, *Eur. Phys. J.* **C63** (2009) 189–285, [arXiv:0901.0002].
- [51] M. Jezabek and J. H. Kühn, *Nucl. Phys.* **B314** (1989) 1.
- [52] M. Cacciari, G. P. Salam, and G. Soyez, *JHEP* **04** (2008) 063, [arXiv:0802.1189].
- [53] S. Biswas, K. Melnikov, and M. Schulze, *JHEP* **1008** (2010) 048, [arXiv:1006.0910].
- [54] A. Kharchilava, *Phys. Lett.* **B476** (2000) 73–78, [hep-ph/9912320].